Computational fluid dynamics applied to study the impact of septal perforations on nasal physiology

Original Article

Authors

Tiago Chantre
Serviço de Otorrinolaringologia, Centro Hospitalar Universitário Lisboa Central, Portugal

Rui Oliveira
Faculdade de Engenharia Mecânica da Universidade do Porto, Portugal

Manuel A. Burgos
Departamento de Ingeniería Térmica y de Fluidos, Universidad Politécnica de Cartagena, Cartagena, Espanha,

Bruno Cunha
Serviço de Neuroradiologia, Centro Hospitalar Universitário Lisboa Central, Portugal,

Mafalda Barroso
Serviço de Otorrinolaringologia, Centro Hospitalar Universitário Lisboa Central, Portugal

Mariana Oliveira
Serviço de Otorrinolaringologia, Centro Hospitalar Universitário Lisboa Central, Portugal,

Ezequiel Barros
Serviço de Otorrinolaringologia, Centro Hospitalar Universitário Lisboa Central, Portugal,

Herédio Sousa
Serviço de Otorrinolaringologia, Centro Hospitalar Universitário Lisboa Central, Portugal.

Correspondence:
Tiago Chantre
tiagomendeschantre@gmail.com

Article received on April 6, 2022.
Accepted for publication on June 27, 2022.

Abstract

Objectives: Use of computational fluid mechanics (MFC) in understanding the impact of the size and location of septal perforations (PS) on nasal physiology
Study design: Computer simulation study.
Material and Methods: MFC software (Flowgy®) was used to create digital models of nasal cavities through computed tomography reconstruction. Virtual surgery was performed with establishment of anterior (1 or 2 cm) and posterior (1 or 2 cm) PS.
Results: Larger perforations cause a greater change in the allocation of airflow regardless of location, with air deviation from the nasal cavity with greater flow to the one with less flow. Bilateral nasal resistance was not significantly altered by the presence of PS.
Conclusions: MFC technologies help to understand how PS change nasal physiology. Airflow allocation is altered, with greater airflow through the less resistant nasal cavity, especially in anterior perforations.
Keywords: Computational Fluid Dynamics, nasal septum, nasal septal perforation, virtual surgery

Introduction

Septal perforations (SPs) are anatomical defects in the nasal septum that create a communication route between the two nasal cavities. Its estimated prevalence is 1–2% among adults[1,2] and 5.4% in patients who undergo septoplasty[3]. In addition to nasal surgery, other risk factors for SPs are trauma with septal hematoma, misused topical nasal medications such as vasoconstrictors, and addiction to inhaled drugs such as cocaine. Perforations can also result from infections and inflammatory or neoplastic diseases[4]. In almost 50% of patients, SPs are idiopathic[4,5]. The most common symptoms are nasal obstruction, epistaxis, crusting, dryness, or nasal pain; approximately 15% of patients are asymptomatic[6].

Septal perforations are classified according to their size and whether their locations are anterior, middle, or posterior, but approximately 92% of SPs are located anteriorly[4]. Perforations that are ≤ 5 mm are often asymptomatic, whereas those ≥ 1 cm are frequently symptomatic[7].

The geometry of the nasal cavities significantly influences airflow behavior and thus affects nasal physiology.[8] Computational fluid mechanics (CFM) have recently emerged as a validated tool for airflow and the effects of medication[9]. Three-dimensional (3D) reconstruction of the nasal cavities from computed tomography (CT) or magnetic resonance images can help simulate airflow patterns, volumetric flow rate (Q), nasal airflow resistance, velocity, pressure, and heat transfer[7,10].

CFM can be applied to routine Ear, Nose and Throat (ENT) clinical practice to improve the quality of diagnosis and treatment as information is provided in addition to that obtained by imaging without a need to expose patients to more radiation or extend the time required for complementary diagnostic tests. The method is widely applied across different disciplines of rhinology as it can predict the impact of nasal septal deviations, inferior turbinate hypertrophy, concha bullosa, or changes in the internal and external nasal valves and simulate their correction by virtual surgery[10]. Other aspects relevant to clinical practice include the impact of uncinectomy on nasal airflow[11].

This study aimed to determine the effects of SPs on nasal physiology using CFM and virtual surgery and the influence of the size and location of SPs on airflow.

Material and Methods

A review of the records of patients whose paranasal sinuses were assessed by CT at the Centro Hospitalar Universitário de Lisboa Central resulted in the selection of a 66-year-old male patient with no changes on CT images, previous nasal surgeries, or a history of brain injury. The results of transnasal fiberoptic laryngoscopy (TNFL) showed that this patient had no nasal irregularities or changes in the nasal mucosa. He was referred to ENT because of a pharyngeal foreign body sensation that had started one year earlier. CT imaging of the paranasal sinuses to investigate thickening of the pharyngeal cavum after TNFL did not reveal any changes. Endoscopy revealed no other abnormal findings. Figure 1 shows a high-resolution CT image of the paranasal sinuses (section thickness, 0.625 mm).

A 3D model was generated from reconstructed CT images (Figure 2) using the CFM software Flowgy®, which also allowed model segmentation and post-processing of the generated mesh. After constructing the original nasal model, SPs were created by virtual surgery. An anterior or posterior three-dimensional bounding box was initially selected in the nasal septum in Flowgy®, in which a circular SP (1 or 2 cm in diameter) was created. We generated five models (Figure 3)— an initial model without SP, two models with anterior SPs of 1 cm and 2 cm in diameter, respectively, and two models with posterior SPs of 1 cm and 2 cm in diameter, respectively.

Figure 1
Coronal CT image of paranasal sinuses in a 66-year-old male

Figure 2
Geometry of 3D model without septal perforation

A simulation was generated for each model, and a constant pressure drop between the atmosphere and the nasopharynx was defined for each simulation to mimic physiological respiration induced by the lungs. The volumetric flow rate was maintained at < 15 L/min to ensure laminar flow. The model was defined as a rigid body to suppress the effect of soft tissue deformation associated with respiration. The exterior (atmospheric) temperature was adjusted to 20°C, and that of the nasal cavities was adjusted to 37°C10.

We analyzed air temperature, pressure, and velocity through different structures of the nasal cavities in six coronal planes obtained from the 3D models. The indices of volumetric flow rate and nasal cavity resistance among the five models were compared.

Results

Air predominantly flowed through the right nasal cavity in the original model without SP (Table 1), and no findings of anamnesis and endoscopy or imaging could explain it. After

Figure 3
Virtual surgery and 3D model.
A - Anterior septal perforation of 1 cm in diameter; B - Anterior septal perforation of 2 cm in diameter; C - Posterior septal perforation of 1 cm in diameter; D - Posterior septal perforation of 2 cm in diameter.

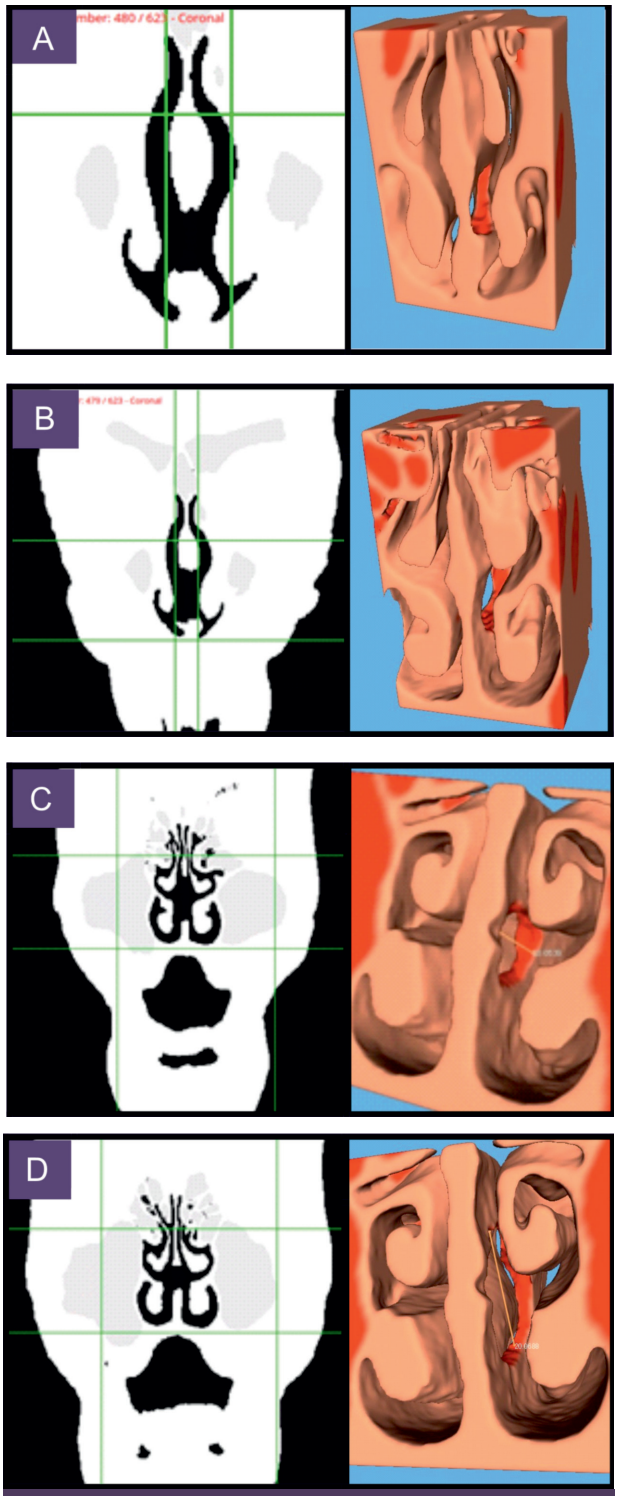

Table 1
Volumetric flow rates (Q; L/min).

No Perforation		Anterior Perforation (1 cm)					Posterior Perforation (1 cm)				
QR	QL	QRB	QRA	QLB	QLA	%Q	QRB	QRA	QLB	QLA	%Q
11.111	3.350	11.373	9.737	3.123	4.760	11,289	11.106	10.084	3.303	4.326	7.096
		Anterior Perforation (2 cm)					Posterior Perforation (2 cm)				
		QRB	QRA	QLB	QLA	%Q	QRB	QRA	QLB	QLA	QLA
		11.821	9.101	3.232	5.308	17.664	11.177	9.101	3.232	5.308	14.408

Volumetric flow rates (Q; L/min) in right (QD) and (QE) left nasal cavities, in right nasal cavity before (QRB) and after (QRA) septal perforation, and in left nasal cavity before (QLB) and (QLA) after septal perforation. %Q, ratio of volumetric flow rate (L/min) through septal perforation.

virtual surgery for the established SPs, the air started flowing through the perforation from the nasal cavity with more flow to that with less. Asymmetric airflow was consistent in all models, with more airflow in the right nasal cavity. A higher volumetric flow rate (%Q) was associated more with anterior than posterior SPs (Table 1)— volumetric flow rates were 62.86% and 81.85% higher, respectively, in anterior than posterior SPs of 1 and 2 cm in diameter. Larger perforations caused greater changes in airflow allocation regardless of their location (Table 1). An increase of 1 cm in the diameter of anterior and posterior SPs, respectively, led to 55.94% and 103.4% increases in the volumetric flow rate.

Resistance (Pa/L/min) remained unchanged in the model with posterior SPs relative to that without SPs, regardless of size (0.602 PA/L/min). Resistance decreased by 3.18% in the anterior SPs when the diameter of the perforation was 2 cm, but this was not statistically significant.

Table 2 shows that an increase in the diameter of anterior and posterior SPs from 1 to 2 cm increased the maximum velocity from 1.955 to 2.200 (13%) and 1.375 to 1.723 m/s (25%), respectively. The velocity was maximal in the central-posterior region of the SPs and minimal in the periphery (mainly at the anterior limit of the SPs). The pattern of heat transfer mimicked that of airflow velocity in both anterior and posterior perforations, but heat exchange was greater in the anterior and larger SPs. However, the SPs did not significantly alter the temperature in the nasopharynx, regardless of size or location (range, 302.821–309.650 °K).

Table 2
Calculation of maximum velocity (m/s) at sites of septal perforation

Septal perforation	Maximum velocity (m/s)
Anterior 1cm	1.955
Anterior 2cm	2.200
Posterior 1cm	1.375
Posterior 2cm	1.723

Discussion

SPs are structural defects in the nasal septum that create a communication pathway between the two nasal cavities. They lead to changes in air flow, which, in turn, are associated with signs and symptoms[12]. As SPs can impact the quality of life, several surgical techniques, from partial or total SP closure to SP enlargement, have been developed to mitigate symptoms[9]. Despite good surgical outcomes of small perforations, septal defects with a diameter > 2 cm are associated with increased technical difficulty. Consensus regarding the optimal procedure or which patients would benefit the most from surgery has not been reached.[13] Here, we investigated changes in nasal physiology caused by SPs of different sizes and locations using digital models of the nasal cavities, CFM, and virtual surgery. We again found that airflow was diverted through the SPs from the side with the highest to that with the lowest flow rate and that the diversion is greater in larger SPs[14]. This defect

was consistent for perforations in all evaluated anatomical locations.

A comparison between anterior and posterior SPs in the CFM models revealed that anteriorly located perforations led to higher airflow velocity, and larger SPs are associated with higher air velocity regardless of location. The ratio (%) of airflow velocity increased according to SP size in the posterior region of the nasal septum. The exact etiology of this phenomenon remains unknown. However, it might be because the conversion from laminar to turbulent airflow is more significant and results in a corresponding increase in velocity when an SP is located in the anterior than the posterior region[14]. These findings might have substantial clinical importance when deciding on the surgical closure of SPs.

Differences in temperature between the surface of the nasal mucosa and inhaled air are important for water transfer to inspiratory air[15]. Li *et al*. showed that SPs alter airflow and impair nasal warming functions[11]. They also showed that patients with larger or anterior perforations had lower airflow temperatures in the nasopharynx. However, these findings have not been confirmed by others[9], and we found that the airflow temperature in the nasopharynx remained unchanged regardless of SP size and location.

CFM allows more detailed diagnostic investigations of SPs and are important for creating individualized treatment plans, thus avoiding unsatisfactory surgical outcomes. As CFM can simulate the parameters of nasal flow assessment before and after virtual closure of SPs, pathological findings other than SPs, such as nasal septal deviation and inferior turbinate hypertrophy, can be considered in advance as contributors to symptoms and changes in nasal airflow[7].

This study has some limitations. The five analyzed models were generated from a single patient. The size (1 or 2 cm in diameter) and the shape (circular) of the perforations were controlled to standardize the models. However, different shapes and anatomical locations of SPs affect airflow and symptoms[9]. Other anatomical aspects such as inferior turbinate hypertrophy or nasal septal deviation were not considered in the models. Nevertheless, this was the only way to reveal the isolated effects of SPs without interference by confounding factors. Translation of a CFM model to the routine clinical setting has a margin of error that should not be underestimated. Although CFM offers a unique opportunity to analyze nasal airflow, many aspects remain enigmatic, and conditions such as empty nose syndrome are typical of the dissociation between CFM findings and symptoms[16]. Therefore, studies to correlate nasal airflow assessed by CFM to the presented symptoms are necessary. These biases mean that definitive conclusions await additional studies of patients with SP and confirmation of the present results.

Conclusions

CFM associated with virtual surgery can help improve the understanding of airflow behavior in the nasal cavities with or without established disease. The SPs altered nasal physiology in our CFM model according to their size or location. Airflow allocation was altered, with more airflow entering the nasal cavity with less resistance, especially in anterior perforations. Larger SPs caused greater changes in airflow allocation regardless of their location.

Conflicts of Interest

The authors declare that there is no conflict of interests regarding the publication of this paper.

Data Confidentiality

The authors declare having followed the protocols in use at their working center regarding patients' data publication.

Protection of humans and animals

The authors declare that the procedures were followed according to the regulations established by the Clinical Research and Ethics Committee and to the 2013 Helsinki Declaration of the World Medical Association.

Funding Sources

This work did not receive any contribution, funding or scholarship.

Availability of scientific data

There are no datasets available, publicly related to this work.

Bibliographic references

1.Oberg D, Akerlund A, Johansson L, Bende M. Prevalence of nasal septal perforation: the Skovde population-based study. Rhinology [Internet] 2003 Jun;41(2):72-5. Available from https://www.rhinologyjournal.com/Rhinology_issues/373.pdf.

2.Gold M, Boyack I, Caputo N, Pearlman A. Imaging prevalence of nasal septal perforation in an urban population. Clin Imaging. 2017 May-Jun;43:80-82. doi: 10.1016/j.clinimag.2017.02.002.

3.Bateman ND, Woolford TJ. Informed consent for septal surgery: the evidence-base. J Laryngol Otol. 2003 Mar;117(3):186-9. doi: 10.1258/002221503321192476.

4.Diamantopoulos II, Jones NS. The investigation of nasal septal perforations and ulcers. J Laryngol Otol. 2001 Jul;115(7):541-4. doi: 10.1258/0022215011908441.

5.Dosen LK, Haye R. Nasal septal perforation 1981-2005: changes in etiology, gender and size. BMC Ear Nose Throat Disord. 2007 Mar 7;7:1. doi: 10.1186/1472-6815-7-1.

6.Lanier B, Kai G, Marple B, Wall GM. Pathophysiology and progression of nasal septal perforation. Ann Allergy Asthma Immunol. 2007 Dec;99(6):473-9; quiz 480-1, 521. doi: 10.1016/S1081-1206(10)60373-0.

7.Burgos MA, Sanmiguel-Rojas E, Rodríguez R, Esteban-Ortega F. A CFD approach to understand nasoseptal perforations. Eur Arch Otorhinolaryngol. 2018 Sep;275(9):2265-2272. doi: 10.1007/ s00405-018-5073-6.

8.Faramarzi M, Baradaranfar MH, Abouali O, Atighechi S, Ahmadi G, Farhadi P, et al. Numerical investigation of the flow field in realistic nasal septal perforation geometry. Allergy Rhinol (Providence). 2014 Jul;5(2):70-7. doi: 10.2500/ar.2014.5.0090.

9.Farzal Z, Del Signore AG, Zanation AM, Ebert CS Jr, Frank-Ito D, Kimbell JS, et al. A computational fluid dynamics analysis of the effects of size and shape of anterior nasal septal perforations. Rhinology. 2019 Apr 1;57(2):153-159. doi: 10.4193/Rhin18.111.

10.Burgos MA, Sanmiguel-Rojas E, Del Pino C, Sevilla-García MA, Esteban-Ortega F. New CFD tools to evaluate nasal airflow. Eur Arch Otorhinolaryngol. 2017 Aug;274(8):3121-3128. doi: 10.1007/ s00405-017-4611-y.

11.Xiong GX, Zhan JM, Zuo KJ, Rong LW, Li JF, Xu G. Use of computational fluid dynamics to study the influence of the uncinate process on nasal airflow. J Laryngol Otol. 2011 Jan;125(1):30-7. doi: 10.1017/S002221511000191X.

12.Li L, Han D, Zhang L, Li Y, Zang H, Wang T. et al. Impact of nasal septal perforations of varying sizes and locations on the warming function of the nasal cavity: A computational fluid-dynamics analysis of 5 cases. Ear Nose Throat J. 2016 Sep;95(9):E9-E14. doi: 10.1177/014556131609500906

13.Passali D, Spinosi MC, Salerni L, Cassano M, Rodriguez H, Passali FM. et al. Surgical treatment of nasal septal perforations: SIR (Italian Society of Rhinology) experts opinion. Acta Otorrinolaringol Esp (Engl Ed). Jul-Aug 2017;68(4):191-196. doi: 10.1016/j.otorri.2016.10.001.

14.Cannon DE, Frank DO, Kimbell JS, Poetker DM, Rhee JS. Modeling nasal physiology changes due to septal perforations. Otolaryngol Head Neck Surg. 2013 Mar;148(3):513-8. doi: 10.1177/0194599812472881.

15.Lindemann J, Leiacker R, Rettinger G, Keck T. Nasal mucosal temperature during respiration. Clin Otolaryngol Allied Sci. 2002 Jun;27(3):135-9. doi: 10.1046/j.1365-2273.2002.00544.x.

16.Balakin BV, Farbu E, Kosinski P. Aerodynamic evaluation of the empty nose syndrome by means of computational fluid dynamics. Comput Methods Biomech Biomed Engin. 2017 Nov;20(14):1554-1561. doi: 10.1080/10255842.2017.1385779.